adsorption after heating to 300.0 °C then cooling to 60.0 °C is consistent with the latter observations.

Madey et al.[7] also report that methane's fraction of the hydrocarbon product at 425 °C (0.99) is considerably higher than this fraction at 175 °C (0.90). It has been suggested that while the methanation mechanism may involve the hydrogenation of a surface carbon species produced by the decomposition of CO, the formation of higher hydrocarbons may require oxygen-containing species as intermediates. This would certainly be consistent with the results of Figure 3. At T = 180.0 °C, for example, considerable adsorbed CO is available from which oxygen-containing species could be formed while at 240.0 °C there is little adsorbed CO and carbon atoms appear to be the predominant surface species.

Care must be taken, however, in extrapolating our results of Figure 3 to other reactant pressure regions, since the corresponding experiments carried out in the 10^{-7} torr range showed a similar type of behavior but the CO band disappears at a temperature approximately 70 °C lower (Figure 4).

References and Notes

(1) P. Mahaffy and M. J. Dignam, *Surf. Sci.*, in press.
(2) M. J. Dignam and J. Fedyk, *Appl. Spectrosc. Rev.*, **14**, 249 (1978).
(3) H. H. Madden, J. Kuppers, and G. Ertl, *J. Chem. Phys.*, **58**, 3401 (1973).
(4) T. N. Taylor and P. J. Estrup, *J. Vac. Sci. Technol.*, **10**, 26 (1973).
(5) M. Araki and V. Ponec, *J. Catal.*, **44**, 439 (1976).
(6) G. A. Mills and F. W. Steffgen, *Catal. Rev.*, **8**, 159 (1973).
(7) T. E. Madey, D. W. Goodman, and R. D. Kelley, *J. Vac. Sci. Technol.*, **16**, 433 (1979).

A Laser-Induced Transient Photovoltaic Effect Using Blocked Electrodes

William F. Coleman,*

Department of Chemistry, University of New Mexico, Albuquerque, New Mexico 87131

Michael G. Prisant, and Richard N. Zare*

Department of Chemistry, Stanford University, Stanford, California 94305 *(Received: May 21, 1980; In Final Form: August 12, 1980)*

An aqueous solution of $KMnO_4$ is irradiated with a pulsed laser source. In the absence of an initially applied voltage, a transient photopotential is observed along the axis of excitation. The sign, magnitude, and temporal dependence of the photopotential are shown to be dependent on, and characteristic of, the nature of the solute. It is shown that the peak potential is linear in the excitation power of the laser source and in the quantum yield for the photoreduction of MnO_4^- as a function of excitation wavelength. It is suggested that the transient potential originates from the photochemical perturbation of the electrode–electrolyte double layer.

Introduction

Traditional electrochemical techniques apply electrical perturbations to a solution and measure the current and/or voltage response of the solution.[1] This study explores the electrical response of solutions to photochemical perturbations in the absence of an initially applied field.

Photovoltaic phenomena are hardly new,[2] but the introduction of the laser to these experiments allows us to reexamine these phenomena in a radically new light.[3,4] We see the following advantages in using a laser to induce a photochemical perturbation in a solution. First, the perturbation is induced in a very short time—on the order of 6–10 ns—with a nitrogen-pumped dye laser. This fine temporal resolution allows us to study rapidly decaying transients formed near the electrode–solution interface with relative ease compared to traditional techniques. Secondly, the laser provides a tunable, narrow excitation frequency. Spectral resolution allows us to deposit a precise amount of energy into a solute and follow its electrochemical behavior as a function of excitation wavelength.

To begin our study of laser-induced photovoltaic phenomena, we chose to measure a transient potential using a blocked electrode because such measurements allow one to isolate the perturbative influence of the light. We selected the permanganate system for detailed study because, after cursorily examining a number of solutes in aqueous solution, we found that the permanganate ion produced the largest value of the peak photopotential. This was a fortunate choice. The photochemistry of MnO_4^- under steady-state photolysis has been studied by several workers[5,6] and, although the mechanism of the photoprocess remains in doubt, Zimmerman[7] has demonstrated that the quantum yield for MnO_4^- photoreduction varies markedly as a function of excitation wavelength.

Experimental Section

Reagents. Reagent grade $KMnO_4$ (Matheson Coleman and Bell) was used without further purification. Solutions were prepared with triply distilled water. All of the results which have been obtained indicate that (1) the permanganate solutions used in this work were stable[8] with respect to decomposition for at least several days and (2) the water used as the solvent contained no species that contributed to the transient photopotentials being measured. In spite of the above, the measurements reported here were made on freshly prepared $KMnO_4$ solutions.

Cell Design. The basic cell design which has been used in this work is shown in Figure 1. The electrodes in the cell are made of NESA glass—SnO_2 coated on borosilicate glass (Practical Products Co.). These electrodes are conducting and optically transparent at wavelengths greater than 310 nm. The electrodes have been coated by vacuum deposition (UVIRA Optics, Mountain View, CA) with a 1–2-μm layer of quartz to prohibit direct contact between the solution under investigation and the SnO_2 surface. Electrical connections are made to evaporated silver contacts on each electrode. The solution being studied is

0022-3654/80/2084-2685$01.00/0

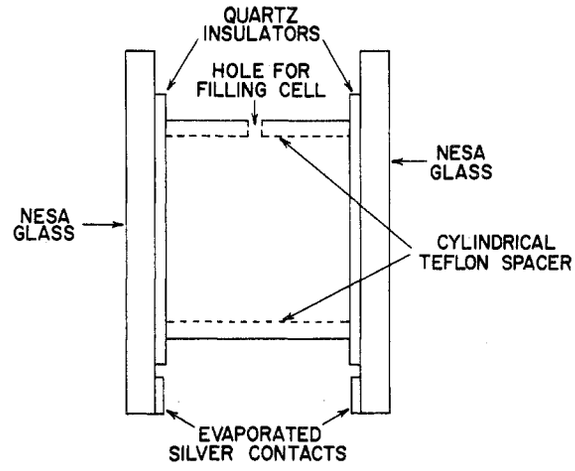

Figure 1. Schematic diagram of the cell used for transient photopotential measurements.

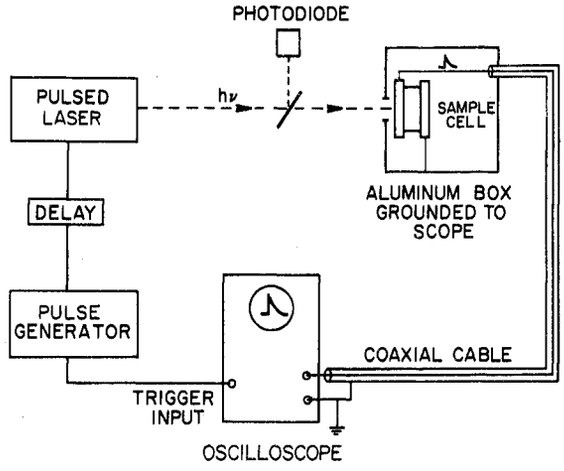

Figure 2. Experimental arrangement for transient photopotential measurements.

contained between the electrodes in a cylindrical teflon spacer. Most of the work here was with a path length of 10 mm. The cell is housed in a shielded aluminum box. The back electrode is grounded to the housing and the signal at the front electrode is input to an oscilloscope which is also grounded to the aluminum box. The limiting factor in the temporal resolution of our experiments is the risetime, 0.5 μs, of the oscilloscope.

Experimental Design. The experimental arrangement is shown in Figure 2. A pulse generator triggers the oscilloscope and then, after a delay of at least 20 μs, triggers a pulsed laser system. The experiment is carried out one pulse at a time. A long quiescent period (several seconds to 5 min) between measurements permits the system to relax completely from one measurement to the next. The lasers which have been employed include an N_2 laser (homemade, 400 kW), an N_2-pumped dye laser (Molectron UV-24, DL14 system), and a YAG-pumped dye laser (Quanta-Ray PDL). All of these lasers have pulse widths of 20 ns or less. The laser dyes used and their respective wavelength ranges were as follows: C495 (515–580 nm), C500 (473–547 nm), C2 (428–465 nm), C120 (420–457 nm), Bis-MBS (411–430 nm), PBBO (391–411 nm), and BBQ (373–399 nm).

Results

Three aspects of the transient signal are readily available in any particular experiment: the magnitude (peak voltage observed on the oscilloscope with a 50-Ω terminator at the input to the oscilloscope), the temporal behavior, and the sign. In the experiments reported here these have been studied as a function of excitation wavelength and laser power.

TABLE I: Transient Photopotentials Observed for Various Aqueous Inorganic Ions and Other Species

photoactive species[a]	λ, nm	ΔJ_{max}, μV
$Co(ox)_3^{3-}$	337	−120
$Fe(ox)_3^{3-}$	337	−205
UO_2^{2+}	337	+100
$Cr_2O_7^{2-}$	337	+105
$Cr(OH_2)_6^{3+}$	450	−120
rhodamine B	337	−245
MnO_4^-	337	−2250

[a] Concentrations varied from species to species and were chosen to give the maximum signal for each species. The concentration dependence of the transient photopotential is a complex function and is a topic of continuing investigation.

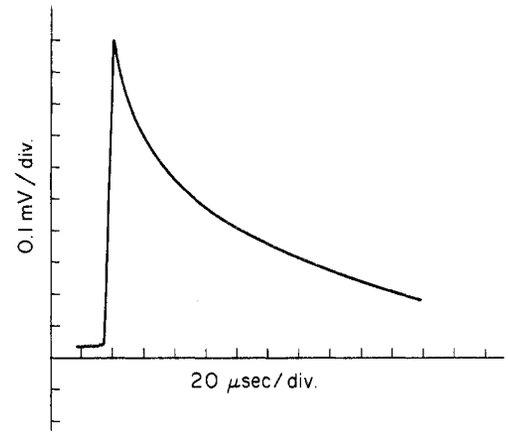

Figure 3. Transient signal observed for 337-nm excitation of 5.2×10^{-4} M MnO_4^-.

The results of several experiments are sufficient to demonstrate that the photovoltages arise from photochemistry of MnO_4^- in the solution and not from some property of the electronics or impurities in the solvent. (1) When the cell is filled with deionized water and pulsed with an unfocused N_2 laser (1.2 mJ/pulse), no transient signal is observed. The detection limit is such that any transient must produce a voltage at the oscilloscope of less than 1 μV to be unobservable. (2) There is no transient produced when nonabsorbing electrolytes such as NaCl or K_2SO_4 are added to the solution. (3) In those cases where a transient photovoltage is observed, the transient can be eliminated completely by blocking the laser beam. (4) Moreover, the sign of the transient signal can be reversed either by rotating the cell by 180° with respect to the laser beam or by reversing the contacts to the electrodes. Consequently, we conclude that the observed transient photovoltages originate from species in solution which absorb the incident laser pulse.

Permanganate ion gives rise to a sizeable photocurrent, producing signals up to several millivolts. Table I lists the maximum signal that has been obtained for several solutes. Because MnO_4^- gave the largest absolute signal, we chose to concentrate on its behavior in this initial study. Figure 3 shows a typical transient signal for MnO_4^- ($[MnO_4^-] = 5.2 \times 10^{-4}$ M) at 25 °C excited with a 337-nm N_2 laser pulse.

When the excitation wavelength is varied, through use of the appropriate laser dyes, the magnitude of the transient photopotential is found to be wavelength dependent. We present in Figure 4 a plot of the wavelength dependence of the photopotential (squares). Each measurement

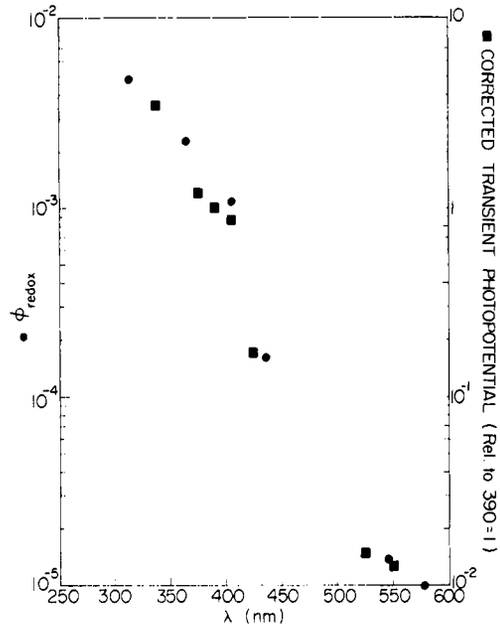

Figure 4. Wavelength dependence of the transient signal (squares) and the photoreduction quantum yield (circles) for MnO_4^-. The quantum yields are from ref 7. The transient signal has been corrected for relative laser power and the fraction of light absorbed. The squares have been normalized to unity at 390 nm.

has been normalized to the same laser intensity and corrected for the fraction of incident light absorbed by the cell and sample at a given excitation wavelength. We also plot in Figure 4 the wavelength dependence of the photoreduction quantum yield, taken from ref 7 (circles). The correspondence between the two types of measurements is striking. The photopotential measurements from 337 to 410 nm were made by using the N_2-pumped dye laser as the excitation source. No signal could be detected at wavelengths greater than 450 nm with this source, and the measurements in the region of the first absorption band in MnO_4^- were performed with the YAG-pumped dye laser as the excitation source. The data in Figure 5 show that the magnitude of the transient is linear with laser power. This fact has been used to correct the data in Figure 4 for variations in power at the different excitation wavelengths. In addition to permitting this correction to be applied, the data in Figure 5 verify that this experiment is monitoring a one-photon process. The fact that the magnitude of the photopotential parallels the photoreduction quantum yield rather than the absorbance of the sample is strong evidence that the phenomenon we are observing arises from solution photochemistry rather than from a thermal perturbation caused by the incident laser pulse.

The temporal behavior of the transient is quite complex. Although this paper will concentrate on the behavior of the peak photovoltage, it should be mentioned that the curve in Figure 3 follows neither a single exponential nor a t^n type decay. This argues against mass transport or double-layer expansion as the origin of the phenomenon.

The data in Figures 3–5 are obtained from the results of fewer than five pulses, with a quiescent period between pulses, on any given solution. Under these conditions less than 1% of the MnO_4^- has undergone photoreduction. Following multiple pulses (>20–30) two phenomena are observed. First, there is an attenuation of the magnitude of the signal, and second a long (1–2 s) tail is observed to grow into the decay of the transient.

The data reported here are from unbuffered solutions of MnO_4^- which contain no supporting electrolyte. Studies in buffered systems at various pH values and with supporting electrolytes up to 0.1 M indicate that the temporal dependence and the magnitude of the photopotential are both functions of the solution composition. However, the type of data shown in Figures 4 and 5 still obtains and the wavelength dependence of the photopotential continues to track the photoreduction quantum yield.

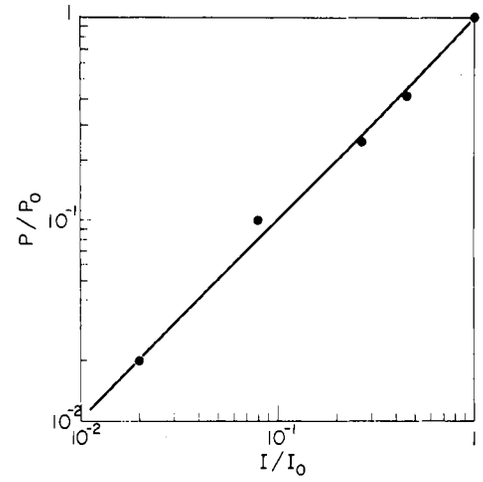

Figure 5. Log–log plot of transient signal magnitude vs. laser power for 5.2×10^{-4} M MnO_4^- excited at 337 nm.

Discussion

We draw the following conclusions from our data: First, reversing the direction of light propagation through the cell reverses the sign of the photovoltage. Thus, the difference in potential between the front and back electrodes, $\Delta\phi$, references the difference of photochemical environment between the front and back electrodes:

$$\Delta\phi = \phi(x=0) - \phi(x=L) \quad (1)$$

where L is the separation between the front and back electrodes.

Second, the peak photovoltage has a linear dependence on the laser power and closely correlates in wavelength dependence with the photoreduction quantum yield. This suggests the concentration of charge near the electrode is proportional to photoproduct concentration. The photoproduct charge concentration is in turn proportional to the intensity $I(x)$ and the quantum yield $\phi(\lambda)$. Hence

$$\Delta\phi \propto [I(x=0) - I(x=L)]\phi(\lambda) \quad (2)$$

In Figure 4 the squares represent $\Delta\phi/[I(x=0) - I(x=L)]$ and it is not surprising then that the squares track $\phi(\lambda)$, represented by circles in Figure 4. We suggest that this method may serve as a new form of actinometry.

Third, the transient photopotential is not due to bulk ion diffusion. The relaxation time scale of the transient is far too short and the magnitude of the signal measured far too large for a diffusion potential. Chemical recombination provides the appropriate time constant for relaxation of the photoproducts, but computer simulation of the superposition of recombination and diffusion does not produce a transient charge separation, and hence a transient potential in a 1-cm path length cell.[9] These arguments also apply to the case of anthracene photoionization in tetrahydrofuran and thus contradict the previous interpretation of Bergman et al.[3] that the photopotential arises from bulk diffusion.

Fourth, the time scale of the transient, microseconds, matches diffusion over a length of $(2Dt)^{1/2} \approx 10^{-5}$ cm or 10^3 Å. This suggests the photopotential originates in the region of the electrode–solution interface and is caused by

photochemical perturbation of the electrode double layer. Double layers are a general consequence of the meeting of two phases at a boundary. The simple existence of a boundary for an electrolyte implies an anisotropy on the forces operating on the particles in the interphase region.[10] There are actually several double layers or electrified interfaces in our experiment: the solution–quartz interface; the quartz–semiconductor interface; and the semiconductor–silver bus bar interface. At the onset of the experiment, the double-layer potentials all cancel. We speculate the laser pulse alters the chemical composition of the electrolyte at the boundary of the cell. Now all the electrified interfaces are still symmetric except the solution interphasial region. Immediately after the light pulse the two electrodes (front and back) find themselves in different chemical environments as a result of the differential absorption of light at the two electrodes.[11] Since the rest of the system remains symmetric, the potential difference $\Delta\phi$ we observe reflects the unrelaxed difference in chemical environment between the two electrodes.

Although this study establishes for the first time a clear relation between photoreduction quantum yield, laser intensity, and observed photopotential, the detailed mechanism how a photochemical perturbation alters the double layer remains unknown, and without such a model we are presently unable to offer an interpretation for the magnitude, sign, and temporal decay of this phenomenon.

Acknowledgment. This work was supported by the National Science Foundation under NSF CHE 78-10019. The use of the YAG laser was made possible through the support of the Stanford Center for Material Research. W.F.C. thanks the Board of Regents of the University of New Mexico for sabbatical leave. M.G.P. thanks NRCC for providing both grant money and guest privileges to pursue computer studies of the phenomena. The authors thank R. P. Van Duyne for helpful discussions regarding electrode properties and dynamics.

References and Notes

(1) D. D. MacDonald, "Transient Techniques in Electrochemistry", Plenum, New York, 1977.
(2) (a) H. W. Russel, *Phys. Rev.*, **32**, 667 (1928); (b) S. Paszyc and R. G. W. Norrish, *Rozn. Chem.*, **37**, 305 (1963).
(3) A. Bergman, C. R. Dickson, S. D. Lidofsky, and R. N. Zare, *J. Chem. Phys.*, **65**, 1186 (1976).
(4) S. P. Perone, J. H. Richardson, B. S. Shepard, J. Rosenthal, J. E. Harter, and S. M. George, *ACS Symp. Ser.*, **No. 85** (1978).
(5) V. Balzani and V. Carassiti, "Photochemistry of Coordination Compounds", Academic Press, New York, 1970.
(6) A. W. Adamson, W. L. Watts, E. Zinayo, D. W. Watts, P. P. Fleischauer, and R. D. Lindholm, *Chem. Rev.*, **68**, 541 (1908).
(7) G. Zimmerman, *J. Chem. Phys.*, **23**, 825 (1955).
(8) R. D. W. Kemmitt and R. D. Peacock, "The Chemistry of Manganese Technology and Rhenium", Vol. 22, Pergamon Press, New York, 1973.
(9) We used a finite difference model to simulate the evolution of charge density $\rho = C_+ - C_-$ and total ion density $\sigma = C_+ + C_-$ in the cell. We approximated the time derivative with the forward difference $D^+_{t,h}v(x,t) = [v(x,t+h) - v(x,t)]/h$ and the second-order space derivative with the centered difference $D^+_{x,l}D^-_{x,l}v(x,t) = [v(x+l,t) - 2v(x,t) + v(x-l,t)]/l^2$. The electroneutrality of the solution $\int_0^c \rho\, dx$ checked the stability of the calculation. We solved for the electric potential by numerical integration of Laplace's equation $d^2\phi/dx^2 = \rho$.
The equations for diffusion in the absence of recombination are analytically tractable. No reasonable photochemical perturbation produces a concentration gradient large enough to separate charge due to the unequal diffusion constants of the positive and negative species and then relax that charge separation on the time scale of the experiment.
The superposition of recombination and diffusion yields an analytically intractable model for the phenomenon. We solved these equations by numerical simulation and found no transient potential.
This has a simple explanation. The time scale for recombination is ~5 orders of magnitude smaller than that for diffusion. Hence, the system recombinatively relaxes the concentration gradient produced by photochemical perturbation well before diffusion can create a charge separation. On the time scale of recombination, there is no bulk diffusion.
(10) J. O'M. Bockris and A. K. N. Reddy, "Modern Electrochemistry", Vol. 2, Plenum Press, New York, 1970, pp 630–632.
(11) In other experiments we used a cell geometry in which the back electrode is not exposed to light. We observed comparable or larger photopotentials.

Magnetic Circular Dichroism and Cryogenic Optical Study of Photochemically Important, Pnictide-Containing Transition Metal Carbonyls

A. F. Schreiner,* S. Amer,† W. M. Duncan,‡ and R. M. Dahlgren§

Departments of Chemistry, North Carolina State University, Raleigh, North Carolina 27650, and University of Toronto, Toronto, Canada; Texas Instruments, Dallas, Texas 75221; and the Proctor and Gamble Company, Cincinnati, Ohio 45247 *(Received: June 24, 1980; In Final Form: August 20, 1980)*

Magnetic circular dichroism (MCD) analysis of pnictide-containing complexes, $[M(CO)_5E]$, where M = Cr or W and E = PPh_3, $AsPh_3$, or $SbPh_3$, gives direct evidence through the presence of a positive A term that the lowest energy, spin-allowed optical band is $^1E \leftarrow {}^1A_1$, of excited configuration $[6e(\sim d_{xz}, d_{yz})]^3[4a_1(\sim d_{z^2})]^1$. The lower ratio of $|A/D|$ for $[Cr(CO)_5E]$ (E = PPh_3, $AsPh_3$, $SbPh_3$) compared to $[Cr(CO)_5(amine)]$ indicates the presence of less orbital angular momentum in the excited state of the former.

For reasons of their diverse photochemical and thermal reaction pathways, photocatalytic activities, photophysics, and frequently encountered high quantum yields of their photoreactions, the 3d 4d, and 5d transition metal carbonyls are a most interesting and important class of molecules.[1] Much of such research either benefits from or demands detailed knowledge of the involved excited state and excited MO, so that we are prompted to present such direct-assignment information from new MCD experimental data and its analysis. Our present results are es-

* Author to whom correspondence should be addressed at the North Carolina State University.
† University of Toronto.
‡ Texas Instruments.
§ North Carolina State University.

0022-3654/80/2084-2688$01.00/0